

BAYSIAN OPTIMASATION OF BLOWING AND SUCTION FOR DRAG REDUCTION ON A TRANSONIC AIRFOIL

F. Mallor¹, A. Frede², S. Rezaeiravesh³, D. Gatti², P. Schlatter^{1,4}

¹*FLOW, Engineering Mechanics, KTH Royal Institute of Technology, Stockholm, Sweden*

²*Institute of Fluid Mechanics, Karlsruhe Institute of Technology (KIT), Karlsruhe, Germany*

³*Department of Fluids and Environment, The University of Manchester, Manchester, UK*

⁴*Institute of Fluid Mechanics (LSTM), Friedrich–Alexander–Universität (FAU),
Erlangen–Nürnberg, Germany*

mallor@kth.se

Abstract

Wall-normal blowing and suction has shown to be a promising active control method for friction drag reduction. In this work, we exploit a Bayesian optimization framework based on Gaussian process regression to find a configuration of non-homogeneous wall-normal blowing and suction capable of improving the aerodynamic efficiency of an RAE2822 airfoil in transonic conditions. The RANS simulations are carried out with the open-source solver SU2. During the optimization process, three different scenarios are considered: only the drag is minimized, the drag and the power needed to drive the control system are included, and the actuation power with a specified compressor efficiency are used for the calculation of the efficiency increase. Even in the most realistic case considering the actuation power and efficiencies an increase in the overall efficiency of 1.15% is reached.

1 Introduction

The CO_2 emissions generated by the aeronautical industry are estimated to be seven times the ones produced by the automotive sector (Mithal and Rutherford, 2023; Kwan, 2013). Therefore, a reduction of these emissions is crucial for mitigating the global warming effects and meeting the global climate goals. According to Airbus estimates (Abbas et al., 2013), the viscous drag associated with direct and indirect losses related to friction is responsible for roughly one-half of the total drag of a commercial airplane. Therefore, even a small reduction of the viscous drag could lead to significant performance improvements, and to a drop in the ecological footprint of the aviation sector. Flow control aimed at reducing the skin-friction drag on solid surfaces immersed in turbulent flows promises to achieve this technological goal by reducing the turbulence contribution to total friction.

Passive control methods like riblets, a particular surface structuring capable of reducing turbulent drag, do not require additional power and may lead to a local drag reduction of about 6% (Walsh et al., 1989) in aeronautic applications. However, in spite of their

success, due to their need for continuous maintenance and their limited drag reduction rates, riblets have only recently been adopted in real-world applications (Lufthansa Group, 2023). Active control strategies, in contrast, do require additional power for sensing or actuation but promise a larger drag reduction potential and net power savings. A number of active strategies have been proposed so far with different degree of complexity and technological readiness, ranging from various wall motions (Ricco et al., 2021) to complex arrangements of actuators and sensors (Cattafesta and Sheplak, 2011).

One aspect of active strategies, limiting their development and adoption in aeronautical applications, is the high complexity of the required actuator and sensor system. Predetermined strategies (Gad-el-Hak, 2000) try to circumvent this limitation by aiming at reducing turbulent skin-friction drag via a predetermined action, thus without the need for additional flow sensing. This comes at the cost of a less targeted use of the control power.

Wall-normal blowing or suction of a small mass flow rate through the surface of an airfoil, object of the present study, has long been considered as a viable predetermined flow control measure thanks to its simplicity and relative ease of integration with the other aeronautic systems. The feasibility and effectiveness of suction in turbulent boundary layers (TBL) to improve performance of high-lift devices was already introduced by Prandtl and Betz (1932) in the 1920s. The first theoretical and experimental investigations on friction drag reduction by blowing in TBL were reported starting from the 1950s Mickley (1954); Black et al. (1958); Romanenko and Kharchenko (1963); Kinney (1967). The first numerical studies in TBL were performed in the early 1990s confirming the strongly pronounced effect of wall transpiration on the local skin friction drag (Piomelli et al., 1991; Sumitani and Kasagi, 1995; Park and Choi, 1999). The corresponding feasibility and potential for compressible flow were shown by Hwang (2004). In recent years, the theoretical drag reduction potential of blowing in

TBL was shown by Kametani and Fukagata (2011) and Stroh et al. (2016) using high-fidelity simulations and focusing on skin-friction drag reduction only.

Compared to the case of semi-infinite zero pressure gradient flat-plate TBL, when wall-normal blowing and suction are considered on airfoils, i.e. in their intended application scenario, more complex effects occur. First, skin-friction drag is not the only drag component on airfoils and therefore does not necessarily need to be the target of successful flow control. Then, airfoil TBLs experience strong pressure gradients and possibly nonequilibrium effects, which may significantly change the response to wall-normal blowing and suction. Moreover, the lift-generating capabilities of airfoils should not be eroded by drag-reducing flow control. Finally, the flow around airfoils in civil general aviation is typically transonic, with weak shock waves occurring on the suction side of the airfoil. Any flow control influence with the shock may significantly affect the airfoil performance in a positive or negative manner.

Some of these aspects have been recently addressed by Atzori et al. (2020) and Fahland et al. (2021), who considered wall-normal homogeneous blowing and suction on a NACA 4412 airfoil via incompressible Reynolds Averaged Navier-Stokes (RANS) and Large Eddy Simulations (LES). They showed that homogeneous blowing and suction can lead to a reduction of the drag coefficient. In particular, Fahland et al. (2021) conducted a detailed RANS parametric study and found that blowing on the pressure side was the most promising configuration in terms of increase of aerodynamic efficiency. Recently, Fahland et al. (2023) revisited the results obtained in Fahland et al. (2021) and showed that no overall net improvement of aerodynamic efficiency is obtained when the effort of providing flow control fluid for blowing or dumping fluid after suction is taken into account.

In the present work, we assess the feasibility of wall-normal blowing and suction for improving the aerodynamic efficiency of a transonic airfoil, i.e. in the presence of compressibility effects and a shock wave, as occurring in real aviation applications. The open scientific questions, as outlined above, are at least two. First, the capability of wall-normal homogeneous blowing and suction to improve the aerodynamic efficiency of airfoils has found contrasting evidence in literature and still requires reliable verification. Second, the compressibility effects and transonic scenario have not been yet investigated thoroughly. In this study, a non-homogeneous wall-normal blowing and suction on the transonic airfoil RAE2822 is investigated. We tackle the wealth of possible blowing and suction arrangement in search of the optimal configuration via a Bayesian optimization based on Gaussian process regression (BO-GPR), with a framework similar to that used by Morita et al. (2022) or by Mahfoze et al.

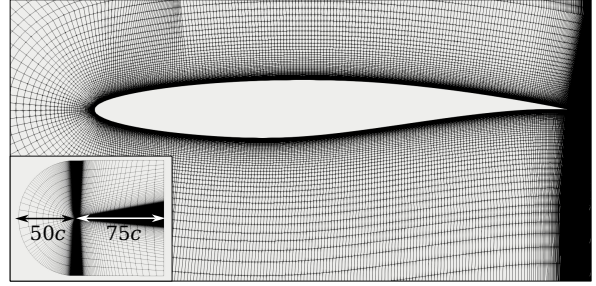


Figure 1: Sketch of the computational mesh utilized in the present study

(2019). The optimizer has the advantage that only a limited number of RANS simulations are required to reach the global optimum.

2 Methodology

The compressible flow around the RAE2822 airfoil of chord length c is simulated using the density-based steady-state RANS solver from the open-source CFD code SU2 (Economou et al., 2016). The $k-\omega$ -SST-model is employed as a turbulence model and a fixed transition point is implemented as a semi-implicit scalar source (Patankar, 1980) at $x/c = 0.1$. The trip location spans 1% of the chord length in streamwise direction and δ_{99} in wall-normal direction. The fluid is modeled as standard air with a constant viscosity. The numerical grid (see Figure 1) consists of hexahedral cells and has a 2D-shaped block pattern. It has a C-radius of $r_c = 50c$ and an outlet distance of $d_o = 75c$.

The airfoil surfaces are modeled as adiabatic walls. In the areas where the active control method is applied, a mass flow is imposed. For regions of blowing, a fixed temperature is prescribed at the wall as described in the following. The velocity and energy fluxes are computed with the thermodynamic properties. The convective fluxes are discretised with the second-order Roe model, whereas for the viscous fluxes the Gauss–Green method was chosen.

The flow is simulated in the transonic regime with a chord-based Reynolds number of $Re = 5.5 \cdot 10^6$ and a Mach number of $Ma = 0.725$. The freestream parameters of the fluid are $T = 216.8$ K, $\rho = 0.365$ kg/m³ and $p = 22715.5$ Pa.

An active control region of wall-normal mass-blowing or suction (also referred to as mass injection or ingestion) is allowed in both the pressure and suction sides starting from $x/c = 0.25$, and spanning up to $x/c = 0.86$. The allowed intensity of the wall-normal massflow (positive for blowing and negative for suction) is limited to 0.25% of the freestream massflow. Two additional constraints are imposed on the optimization: the total length of the blowing region must be at least 10% of the chord, and the sum of the total suction and blowing massflows must be the same so that the overall active control results in

zero net mass flux. The former is used to avoid major discontinuities in the solution, which could undermine stability and whose effect can hardly be captured by RANS simulations. The latter constraint was imposed in order to study a self-contained flow control system, in which no additional air must be supplied or exhausted from the free-stream. In order to estimate the power of the actuation, we consider a simplified system in which a single compressor (or turbine) connects the suction and blowing regions. The power required to operate the control system can be computed as the mass flowing across the compressor times the change in total enthalpy (Δh_t). Using the isentropic relations, the expression can be rearranged to depend on the total pressure ratio across the compressor and the inflow temperature:

$$P_{s \rightarrow b} = \dot{m} c_p T_{t,s} \left(\left(\frac{p_{t,b}}{p_{t,s}} \right)^{\frac{\gamma-1}{\gamma}} - 1 \right) \quad (1)$$

where c_p is the specific heat constant, γ the specific heat ratio, \dot{m} the massflow, $T_{t,s}$ the suction air temperature and $p_{t,b}$ and $p_{t,s}$ the blowing and suction pressures, respectively. The pressure ratio is given by the regions in which the flow control is applied: $p_{t,b}$ is taken as the maximum pressure of the blowing region, whereas $p_{t,s}$ is fixed from the point of minimum pressure of the suction region. Moreover, the efficiency (η) of the compressor can be taken into account easily: $P_\eta = P/\eta$. In the present work, three different cases are considered:

- **min(c_D)**: Only the drag is accounted for in the maximization of the efficiency;
- **min($c_D + c_P$)**: Both drag and the power needed to drive the control actuation are used in the denominator of the efficiency ($E_{power} = c_L/(c_D + c_P)$);
- **min($c_D + c_{P_\eta}$)**: The actuation power is computed assuming a compressor efficiency (η) equal to 0.8.

Lastly, the temperature at the outlet of the compressor is prescribed as a fixed value boundary condition for the region in which blowing is applied. The temperature is computed using the isentropic relations and the pressure ratio across the compressor as follows:

$$T_{t,b} = T_{t,s} \left(\frac{p_{t,b}}{p_{t,s}} \right)^{\frac{\gamma-1}{\gamma}} \quad (2)$$

A surrogate model of the aerodynamic response as a function of the prescribed control actuation parameters is built using a Gaussian Process Regression (GPR (Rasmussen and Williams, 2006)) with the open-source library GPy (see reference (gpy, 2012)). The parameters of the GPR (with a Matern52 kernel for the covariance function) are fitted using the available observations obtained by simulating the flow with

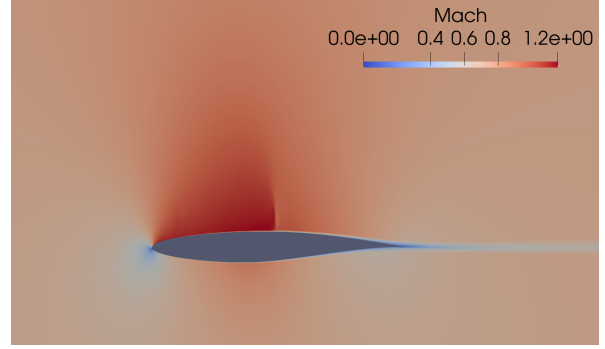


Figure 2: Distribution of the local Mach number around the airfoil for the reference simulation without active control.

some prescribed control boundary conditions (BC) in SU2. Moreover, in order to accelerate convergence, we impose the symmetry inherent in the problem by interchanging the beginning and end points (*i.e.* at each iteration, two values are stored: the original one, and one in which the start and end point values are swapped).

In order to draw the sequence of training samples (*i.e.* the parameter of the control schemes to be simulated next), the expected improvement (EI) acquisition function is maximized (for a detailed description of the EI function and its application to GPR, we refer the reader to the second section in the work by Morita et al. (2022)). Using a hyper-parameter ξ , a balance between exploration (minimizing parts of the parameter space with high variance), and exploitation (maximizing the use of the best objective) is established. In the present case, we set $\xi = 1 \cdot 10^{-3}$. For the GPR-BO, the library GPyOpt (see reference gpy, 2016) is used.

In the present work, the aerodynamic characteristics of the uncontrolled airfoil at an angle of attack (α) of 2° are used as a baseline in order to compare the effectiveness of the control actuation. In this baseline case (see Figure 2), the lift (c_L) and drag (c_D) coefficients are equal to $6.38 \cdot 10^{-1}$ and $9.89 \cdot 10^{-3}$, respectively, giving an aerodynamic performance ($E = c_L/c_D$) of 64.5. The objective is to increase the aerodynamic performance while maintaining the same lift force (*i.e.* reducing c_D). This is achieved by correcting the angle of attack using a Newton method implemented into SU2 until the c_L matches the baseline in each of the studied control cases.

3 Results

For each of the three optimization scenarios 50 simulations were carried out and the aerodynamic performances obtained for the best cases found in each of them are reported in Table 1. The evolution of the response (objective of the minimization) is shown in Figure 3. As seen in the right panel, the optimal response was found earlier than the 50th iteration in all cases. From that point on, the optimization pro-

Table 1: Aerodynamic properties and power consumption of the optimal control strategies.

Case	AoA	c_D	c_P	\dot{m}_c	E	E_{power}
Baseline	2.0	$9.89 \cdot 10^{-3}$	0.0	0.0	64.50	-
$\min(c_D)$	1.41	$9.31 \cdot 10^{-3}$	$2.90 \cdot 10^{-3}$	11.89	68.48	52.22
$\min(c_D + c_P)$	1.92	$9.65 \cdot 10^{-3}$	$1.12 \cdot 10^{-4}$	1.37	66.11	65.35
$\min(c_D + c_{P_\eta})$	1.88	$9.60 \cdot 10^{-3}$	$1.74 \cdot 10^{-4}$	2.21	66.43	65.24

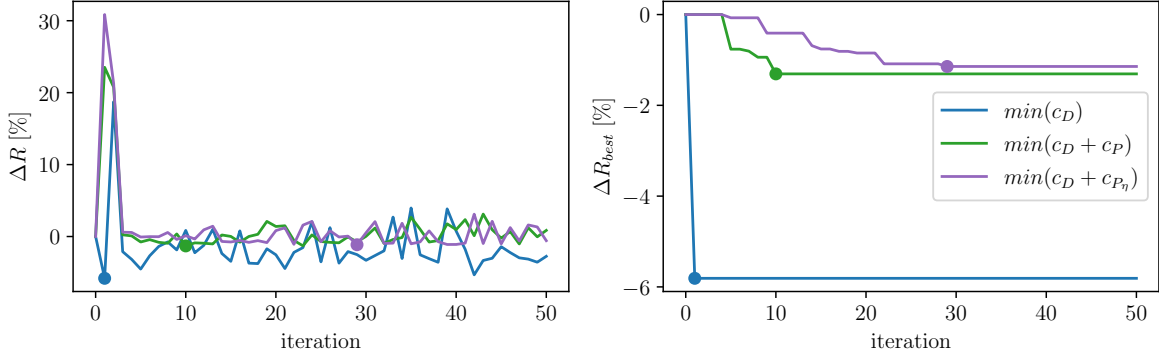


Figure 3: Evolution of the response (as a relative percentage change versus the baseline case) with the number of iterations (left) and cumulative best response found (right).

cess explored the parameter space and reduced the uncertainty around the point of maximum power efficiency gain. As the complexity of the objective function increases (by taking into account the control actuation power, and efficiency), the number of iterations needed to reach the optima increases. Given the complexity of the cases (the presence of a shock, the requirement to maintain a constant c_L), and the number of optimization parameters, the fact that convergence to an optimal strategy was achieved in such few flow realizations supports the effectiveness and robustness of BO-GPR as a flow optimization tool. Moreover, the method works as a black box and is non-intrusive, i.e. it does not require to perform any sort of adjoint or gradient computations within the numerical simulation.

As shown in Figure 4, all control configurations which lead to an increase in the aerodynamic efficiency share a common feature across the different optimization: mass-flow ingestion (suction) takes place on the suction side, while mass-flow (blowing) is injected into the pressure side. Clear differences in the optimal control actuations appear once the power, and not just the drag, is taken into account in the efficiency calculation: For the $\min(c_D)$ case, the control is applied at its maximum allowed strength over the whole admissible control region. The strong suction over the span of the suction side leads to a more attached flow, causing the circulation around the airfoil to increase, and hence increasing its lift coefficient. As the lift coefficient is fixed, this in turn leads to a decrease in the angle of attack required to obtain the required lift. The reduction in angle of attack (1.4° versus the baseline 2°) results in a downstream shift of the position of the shockwave which (clearly seen both in the

pressure and friction coefficient distributions shown in Figure 5), together with the reduction in friction drag over the pressure side due to blowing (see the right plot of Figure 5), leads to a substantial reduction in the drag coefficient: The aerodynamic efficiency improves by 6.2%. However, as the power depends directly on the maximum pressure ratio across the two control regions, sucking air from the position upstream of the shockwave (where the pressure ratio is high) is not power-efficient, which translates into a decrease of E_{power} compared to the baseline case (see Table 1), i.e. no net power saving can be achieved. This feature is clearly reflected in the optimal control actuations found for the cases in which the power actuation was part of the optimization objective: as seen in Figure 4 no suction is performed before the position of the shock. This leads to a smaller downstream shift of the shockwave (around 1.5 versus 4% of the chord for the previous case), resulting in more moderate gains in terms of the aerodynamic efficiency. On the other hand, the actuation over the pressure side remains virtually unchanged, as the air ingested in the suction side is exhausted uniformly over the control region on the pressure side. Even though the gains in power efficiency are moderate (1.32 and 1.15% for the case with η equal to 1 and 0.8, respectively), the optimal actuation strategies still yield an increased aerodynamic performance when compared to the baseline case, which has not been observed in previous studies.

While RANS convergence for the aerodynamic coefficients after 30000 iterations is well below the significant digits reported here, the modeling error due to RANS may be larger than the small performance improvement margin measured in the present study for

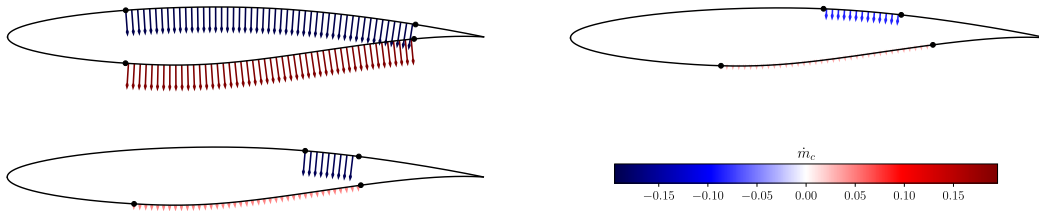


Figure 4: Best control strategy found after the optimization process for the case in which the drag is minimized (top left), and for the cases in which the cost of the control actuation is taken into account in the objective function (top right and bottom left represent the cases with η equal to 1 and 0.8 respectively).

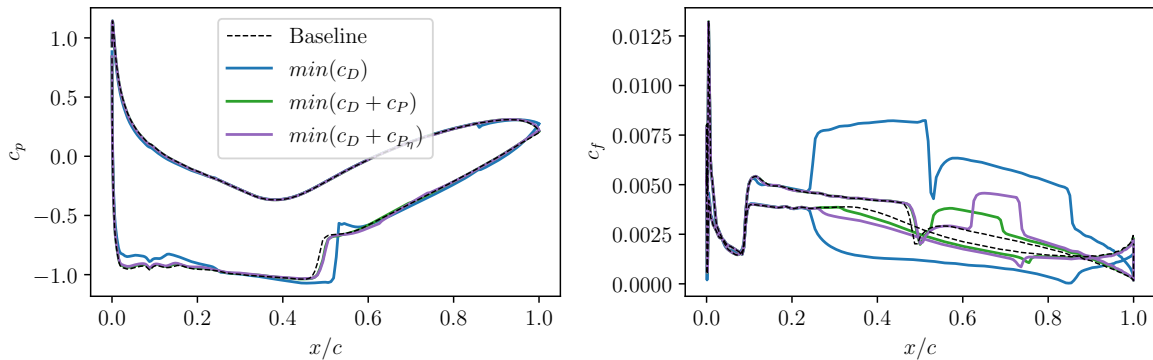


Figure 5: Pressure c_p (left) and skin-friction c_f coefficient (right) obtained after the optimization process. The baseline case is represented with a black, dashed line, the best control strategy with a solid lines. The color coded refers to the three considered optimization cases as reported in the legend.

such complex flow scenario. A more robust verification of the present results through well-resolved LES is planned. If included into the multifidelity framework developed by Rezaeiravesh et al. (2023), the results of more accurate LES simulations will not only serve as validation but can be utilized to improve the whole surrogate model of the aerodynamic response.

Besides the current uncertainty related to the RANS simulations, the present results show that improving the aerodynamic efficiency via wall-normal blowing and suction is theoretically possible, also when the ideal cost of the active control strategy is taken into account. We were able to achieve this results thanks to a Bayesian optimization framework, which could find the optimal blowing and suction configurations within the very large parameter space. The small improvement in net aerodynamic efficiency should not surprise. On the one hand, the airfoil shape is already optimized for the cruise flight at the reference conditions. A holistic approach, in which both the airfoil shape and active control are designed and optimized together could yield better results. On the other hand, we limited ourselves to considering active control in the turbulent region of the airfoil. Possible future work could combine blowing for skin-friction reduction in the TBL with suction (see, e.g., Beck et al., 2018) on the suction side for delaying laminar-

turbulent transition. The larger drag saving owing to the later transition combined with a better investment of the ingested fluid for blowing in the TBL could deliver much higher overall performance of the active control via blowing and suction.

Acknowledgments

FM and PS acknowledge the funding from the Knut and Alice Wallenberg Foundation. DG and AF acknowledge the support of the Boysen Foundation. The simulations were performed on resources provided by the National Academic Infrastructure for Supercomputing in Sweden (NAISS) at PDC (KTH Royal Institute of Technology).

References

- Gpy. <https://github.com/SheffieldML/GPy>, 2012.
- Gpyopt. <https://github.com/SheffieldML/GPyOpt>, 2016.
- A. Abbas, J. de Vicente, and E. Valero. Aerodynamic technologies to improve aircraft performance. *Aerospace Science and Technology*, 28(1):100–132, July 2013. ISSN 1270-9638.
- M. Atzori, R. Vinuesa, G. Fahland, A. Stroh, D. Gatti, B. Frohnapfel, and P. Schlatter. Aerodynamic effects of uniform blowing and suction on a NACA4412 airfoil. *Flow, Turbulence and Combustion*, 105(3):735–759, 2020.

- N. Beck, T. Landa, A. Seitz, L. Boermans, Y. Liu, and R. Radespiel. Drag Reduction by Laminar Flow Control. *Energies*, 11(1):252, 2018. ISSN 1996-1073.
- T. J. Black, A. J. Sarnecki, and W. A. Mair. *The turbulent boundary layer with suction or injection*, volume 20. ARC Cambridge, UK, Cambridge, UK, 1958.
- L. N. Cattafesta and M. Sheplak. Actuators for Active Flow Control. *Annual Review of Fluid Mechanics*, 43(1):247–272, 2011. doi: 10.1146/annurev-fluid-122109-160634.
- T. Economon, F. Palacios, S. Copeland, T. Lukaczyk, and J. Alonso. SU2: An open-source suite for multiphysics simulation and design. *AIAA Journal*, 54(3):828–846, 2016.
- G. Fahland, A. Stroh, B. Frohnapfel, M. Atzori, R. Vinuesa, P. Schlatter, and D. Gatti. Investigation of blowing and suction for turbulent flow control on airfoils. *AIAA Journal*, 59(11):4422–4436, 2021.
- G. Fahland, M. Atzori, A. Frede, A. Stroh, B. Frohnapfel, and D. Gatti. Drag assessment for boundary layer control schemes with mass injection. *Flow, Turbulence and Combustion*, accepted for publication, 2023.
- M. Gad-el-Hak. *Flow Control – Passive, Active and Reactive Flow Management*. Cambridge University Press, Cambridge, 2000.
- D. Hwang. Review of research into the concept of the microblowing technique for turbulent skin friction reduction. *Progress in Aerospace Sciences*, 40(8): 559–575, November 2004. ISSN 03760421. doi: 10.1016/j.paerosci.2005.01.002.
- Y. Kametani and K. Fukagata. Direct numerical simulation of spatially developing turbulent boundary layers with uniform blowing or suction. *J. Fluid Mech.*, 681:154–172, August 2011. ISSN 0022-1120, 1469-7645. doi: 10.1017/jfm.2011.219.
- R. B. Kinney. Skin-friction drag of a constant-property turbulent boundary layer with uniform injection. *AIAA Journal*, 5(4):624–630, April 1967. ISSN 0001-1452, 1533-385X. doi: 10.2514/3.4039.
- I. Kwan. Planes, trains, and automobiles: Counting carbon. Technical report, International council on clean transportation, September 2013.
- Lufthansa Group. When nature acts as a role model: Lufthansa group and basf introduce sharkskin technology, 2023.
- O. A. Mahfoze, A. Moody, A. Wynn, R. D. Whalley, and S. Laizet. Reducing the skin-friction drag of a turbulent boundary-layer flow with low-amplitude wall-normal blowing within a Bayesian optimization framework. *Physical Review Fluids*, 4(9):094601, 2019.
- H. S. Mickley. Heat, mass, and momentum transfer for flow over a flat plate with blowing or suction. *NACA, TN 3208*, pages 1–25, 1954.
- S. Mithal and D. Rutherford. ICAO’s 2050 net-zero CO2 goal for international aviation. Technical report, International Council on Clean Transportation, January 2023.
- Y. Morita, S. Rezaeiravesh, N. Tabatabaei, R. Vinuesa, K. Fukagata, and P. Schlatter. Applying Bayesian optimization with Gaussian process regression to computational fluid dynamics problems. *Journal of Computational Physics*, 449:110788, 2022. ISSN 0021-9991.
- J. Park and H. Choi. Effects of uniform blowing or suction from a spanwise slot on a turbulent boundary layer flow. *Physics of Fluids*, 11(10):3095–3105, October 1999. ISSN 1070-6631, 1089-7666. doi: 10.1063/1.870167.
- S. V. Patankar. *Numerical Heat Transfer and Fluid Flow*. Series in Computational Methods in Mechanics and Thermal Sciences. Hemisphere Publ. Co, New York, 1980. ISBN 978-0-89116-522-4. OCLC: 31743097.
- U. Piomelli, P. Moin, and J. Ferziger. Large eddy simulation of the flow in a transpired channel. *Journal of Thermophysics and Heat Transfer*, 5(1):124–128, January 1991. ISSN 0887-8722, 1533-6808. doi: 10.2514/3.238.
- L. Prandtl and A. Betz, editors. *Ergebnisse der Aerodynamischen Versuchsanstalt zu Göttingen - IV. Lieferung*, volume 7 of *Göttinger Klassiker der Strömungsmechanik*. Göttingen University Press, Göttingen, 1932. ISBN 978-3-941875-42-5. doi: 10.17875/gup2009-104.
- C. E. Rasmussen and C. K. I. Williams. *Gaussian Processes for Machine Learning*, volume 20. the MIT Press, Massachusetts Institute of Technology, 2006.
- S. Rezaeiravesh, T. Mukha, and P. Schlatter. Efficient prediction of turbulent flow quantities using a bayesian hierarchical multifidelity model. *Journal of Fluid Mechanics*, 964:A13, 2023.
- P. Ricco, M. Skote, and M. A. Leschziner. A review of turbulent skin-friction drag reduction by near-wall transverse forcing. *Prog. Aero. Sci.*, 123:100713, May 2021. ISSN 0376-0421. doi: 10.1016/j.paerosci.2021.100713.
- P. N. Romanenko and V. N. Kharchenko. The effect of transverse mass flow on heat transfer and friction drag in a turbulent flow of compressible gas along an arbitrarily shaped surface. *International Journal of Heat and Mass Transfer*, 6(8):727–738, August 1963. ISSN 00179310. doi: 10.1016/0017-9310(63)90043-7.
- A. Stroh, Y. Hasegawa, P. Schlatter, and B. Frohnapfel. Global effect of local skin friction drag reduction in spatially developing turbulent boundary layer. *J. Fluid Mech.*, 805:303–321, October 2016. ISSN 0022-1120, 1469-7645. doi: 10.1017/jfm.2016.545.
- Y. Sumitani and N. Kasagi. Direct numerical simulation of turbulent transport with uniform wall injection and suction. *AIAA Journal*, 33(7):1220–1228, July 1995. ISSN 0001-1452, 1533-385X. doi: 10.2514/3.12363.
- M. J. Walsh, W. L. Sellers III, and C. B. Mcginley. Riblet drag at flight conditions. *Journal of Aircraft*, 26(6):570–575, 1989.